Effects of Iron Status on Transpulmonary Transport and Tissue Distribution of Mn and Fe

Joseph D. Brain, Elizabeth Heilig, Thomas C. Donaghey, Mitchell D. Knutson, Marianne Wessling-Resnick, and Ramon M. Molina

Department of Environmental Health, and Department of Genetics and Complex Diseases, Harvard School of Public Health, Boston, Massachusetts; and Department of Food Science and Human Nutrition, University of Florida, Gainesville, Florida

Manganese transport into the blood can result from inhaling metal-containing particles. Intestinal manganese and iron absorption is mediated by divalent metal transporter 1 (DMT1) and is upregulated in iron deficiency. Since iron status alters absorption of Fe and Mn in the gut, we tested the hypothesis that iron status may alter pulmonary transport of these metals. DMT1 expression in the lungs was evaluated to explore its role in metal transport. The pharmacokinetics of intratracheally instilled ^{54}Mn or ^{59}Fe in repeatedly bled or iron oxide–exposed rats were compared with controls. Iron oxide exposure caused a reduction in pulmonary transport of ^{54}Mn and ^{59}Fe, and decreased uptake in other major organs. Low iron status from repeated bleeding also reduced pulmonary transport of iron but not of manganese. However, uptake of manganese in the brain and of iron in the spleen increased in bled rats. DMT1 transcripts were detected in airway epithelium, alveolar macrophages, and bronchial-associated lymphoid tissue in all rats. Focal increases were seen in particle-containing macrophages and adjacent epithelial cells, but no change was observed in bled rats. Although lung DMT1 expression did not correlate with iron status, differences in pharmacokinetics of instilled metals suggest that their potential toxicity can be modified by iron status.

Keywords: anemia; DMT1; iron status: manganese; transport

Breathing mixtures of metals is common. Ambient metal-containing particles from fuel combustion and other industrial sources can be significant sources for inhalation. Some occupations, such as welding, have greater inhaled metal exposure. Extended exposures to high concentrations of metal-containing particles can produce toxic effects. In particular, inhalation exposure to manganese-containing materials can result in manganism, a Parkinson's-like neurological disorder (1, 2). Understanding the fate of metals contained in inhaled particles that deposit in the lungs is essential in evaluating health effects of metals in the environment. Divalent metals such as Fe, Mn, Pb, Ni, Cu, and Co may share common transport systems such as divalent metal transporter 1 (DMT1) (3). Different metallic ions may interact and thus their absorption through the lungs may be altered.

Iron absorption from the gut is a regulated mechanism, mainly influenced by iron stores in the body. In iron deficiency anemia, iron and manganese absorption in the duodenum is enhanced primarily by upregulation of DMT1 (3–5). Varying the levels of iron in oral dosages has been shown to influence the percent of manganese absorbed (6). Moreover, manganese uptake into the brain is increased during iron deficiency (7, 8). In contrast, dietary iron overload diminishes manganese accumulation in the brain. Iron status varies significantly among the population (e.g., severely anemic individuals versus welders who chronically breathe iron). Thus, relative risks of toxic effects from pulmonary absorption of manganese may differ within the population. Two hypotheses are that (*1*) iron and manganese share common carrier transport systems in the respiratory and gastrointestinal tracts, and (*2*) these systems may be downregulated in individuals who consume an iron-rich diet or have high iron levels in their lungs. Iron and manganese may share ion transport system(s) in the respiratory system as in the gastrointestinal tract (9, 10). To examine whether iron status affects transport of manganese through the lungs, we manipulated iron status in a rodent model by repeated bleeding or by introducing iron oxide particles into the lungs. We then examined the fate of instilled radioactive manganese and iron as well as the expression of the metal transporter protein, DMT1.

MATERIALS AND METHODS

Experimental Animals

Male virus-antigen–free (VAF) CD rats were obtained from Harlan Sprague-Dawley (Indianapolis, IN). They were acclimatized for a few days before the experiments. All procedures were approved by Harvard Institutional Animal Care and Use Committee. The rats were randomly divided into three groups: (*1*) normal control, (*2*) repeatedly bled, and (*3*) iron oxide aerosol exposed or instilled rats. To reduce iron status, rats were repeatedly bled by removal of 0.1 ml blood per kg body weight (15% of estimated blood volume) three times before the pharmacokinetic studies. The protocol consisted of bleeding via the retro-orbital sinus at 7, 5, and 3 d before the experiment. To increase pulmonary content of iron, rats for ^{54}Mn pharmacokinetic study were exposed to iron oxide fumes (AMMD of 0.68 μm) generated by the combustion of iron pentacarbonyl vapor (11). The animals were exposed to the fumes, approximately 100 mg/m^3, inside a Plexiglas chamber for 4 h, five times over a 2-wk period before the metal uptake experiments. Alternatively, rats for ^{59}Fe pharmacokinetic study were intratracheally instilled with a suspension of iron oxide particles at a dose of 7.5 mg/kg every 3 d for a total of five instillations (12). Briefly, rats were placed on a slanted platform while anesthetized with vaporized Halothane (Halocarbons Lab, Inc., North Augusta, SC) and supported by an elastic band placed under the upper incisors. The iron oxide particle suspension was delivered to the lungs via a blunt 18-gauge needle inserted between the vocal chords and into the trachea. Transillumination of the larynx was provided by a microscope lamp shining on the neck (12). Since the rats were exposed to iron oxide by either aerosol exposure or iron oxide particle instillation, the total deposited dose and its distribution might be different. Indeed, the distribution of aerosol-delivered particles is

(*Received in original form March 11, 2005 and in final form October 28, 2005*)

This work was supported by NIH grants ES-000002, (J.D.B), DK60528 (M.W.-R.), DK09998 (M.D.K.), and a gift from the American Welding Society (J.D.B.). The sponsors of this research were not involved in study design, execution, or interpretation of results and were not involved in the decision to submit this paper for publication. Additional support for the interpretation of results and authorship of this publication was made possible by P01 ES012874 from the National Institute of Environmental Health (NIEHS/NIH), and from a STAR Research Assistance Agreement No. RD-83172501 awarded by the U.S. Environmental Protection Agency (EPA). It has not been formally reviewed by either the NIEHS or EPA. The views expressed in this document are solely those of the authors and do not necessarily reflect those of either the NIEHS or the EPA. Neither the NIEHS nor the EPA endorses any products or commercial services mentioned in this publication.

Correspondence and requests for reprints should be addressed to Ramon M. Molina, Department of Environmental Health, Harvard School of Public Health, 665 Huntington Ave., Boston, MA 02115. E-mail: rmolina@hsph.harvard.edu

Am J Respir Cell Mol Biol Vol 34. pp 330–337, 2006
Originally Published in Press as DOI: 10.1165/rcmb.2005-0101OC December 9, 2005
Internet address: www.atsjournals.org

more uniform than instilled particles (12). The deposited doses were likely to be similar from estimates of deposited dose based on aerosol exposure and ventilation parameters. Nonheme iron measurements (Table 1) confirmed that retained iron was within approximately 40% for both inhalation (1.13 mg/g lung) and instillation (1.95 mg/gm). At the end of each procedure to modify iron status, rats from each group were studied to (*1*) determine nonheme iron concentration in lungs, liver, and brain; (*2*) determine lung DMT1 expression by performing in situ hybridization or RT-PCR; (*3*) determine the toxic and inflammatory effects of each treatment; and (*4*) determine the pulmonary absorption and tissue distribution of intratracheally instilled ^{54}Mn or ^{59}Fe.

Nonheme Iron Determination

Frozen lung, liver, and brain samples were thawed and aliquots were weighed. Samples (50–100 μg) were acid hydrolyzed in 2 ml of a mixture of equal volumes of 6-N-hydrochloric acid and 20% trichloroacetic acid at 65°C for 20 h. After cooling to room temperature, the clear yellow solution was transferred to a test tube and a color reagent (0.1% sulphonated bathophenanthroline mixed with 1% thioglycolic acid and distilled water at 1:25:25 ratio) was added. After a 10-min incubation, the optical density was measured at 540 nm. A standard curve was prepared using an iron standard solution (VWR). Nonheme iron in tissue was calculated based on the standard curve, and expressed as μg/g wet tissue. This procedure is described in detail elsewhere (13).

Bronchoalveolar Lavage and Analysis

Three days after the last bleeding and 1 wk after the last iron oxide aerosol exposure, rats were humanely killed by intraperitoneal injection of a lethal dose (200 mg/kg) of pentobarbital sodium (Anthony Products Co., Arcadia, CA). The abdomen was subsequently opened, the hemidiaphragm punctured to create a bilateral pneumothorax, and the abdominal aorta cut to exsanguinate the rat. The trachea was exposed and cannulated. The lungs were lavaged 12 times *in situ* with 3-ml washes of sterile 0.9% saline. The first two washes were pooled for biochemical assays. Cells were separated from the supernatant in all washes by centrifugation (400 × *g* at 4°C for 10 min). Total and differential cell counts and hemoglobin measurements were made from the cell pellets. The supernatant fraction of the first two washes was clarified by centrifugation at 15,000 × *g* for 30 min and used for measurement of enzyme activities and albumin concentration. Standard spectrophotometric assays were used for lactate dehydrogenase (LDH), myeloperoxidase (MPO), and albumin (14).

^{54}Mn or ^{59}Fe Pharmacokinetics

Rats from each treatment group were weighed and then instilled with $^{54}MnCl_2$ (7.5 μCi/kg) or $^{59}FeCl_3$ (16 μCi/kg). $^{54}MnCl_2$ solution was prepared in sterile pyrogen-free saline (final concentration of 0.0007 μg ^{54}Mn/ml), and instilled intratracheally in anesthetized rats at a volume dose of 1.5 ml/kg. To reduce ^{59}Fe to the ferrous form, $^{59}FeCl_3$ stock was diluted 1:4,000 (vol/vol) in 10 mM sodium ascorbate (final concentration of 0.6 μg ^{59}Fe/ml). Radioactive manganese and iron were delivered to the lungs through the trachea as described earlier in this article and as detailed elsewhere (12). Rats were then placed in metabolic cages with food and water *ad libitum*. Blood samples (∼ 50 μl) were collected from the tail artery at 5, 15, and 30 min, and at 1, 2, and 4 h after instillation. Five rats from each group were humanely killed at 4 h. Rats were dissected and the lungs, brain, heart, spleen, kidney, gastrointestinal tract, liver, and samples of skeletal muscle and bone marrow were collected, weighed, and placed in tubes. Urine and fecal samples were also collected. A similar cohort of manganese-instilled rats was humanely killed at 72 h. Radioactivity was measured in a Packard gamma counter (Cobra Quantum; Packard Instrument, Meriden, CT). Disintegrations per minute were calculated from the counts per minute and the counter efficiency. Data were expressed as μCi/g tissue as well as the percentage of the instilled dose retained in each organ. The radioactivity in organ and tissue activity not measured in their entirety was estimated (as a percentage of total body weight) as follows: skeletal muscle, 45%; bone marrow, 3%; and peripheral blood, 7% (15–17).

In Situ Hybridization

After rats were killed, the tracheas were cannulated with a blunt 18-gauge needle connected to a syringe filled with O.C.T. (optimum cutting temperature) compound (Sakura Finetek U.S.A., Torrance, CA) prewarmed to 37°C. Lungs were filled with O.C.T., cut laterally into sections, mounted in O.C.T., snap-frozen in 2-methylbutane chilled on dry ice, and stored at −80°C. Ten-micrometer-thick sections were cut on a cryotome and stored at −20°C until processed. *In situ* hybridization was performed as described elsewhere (3). Briefly, digoxigenin-labeled sense and antisense cRNA probes were transcribed from a rat DMT1 cDNA fragment (bases 105–1,788) flanked by T7 and SP6 promoter sites. Transcripts were shortened to an average length of 200–400 bp by alkali hydrolysis. Sections were incubated with sense or antisense probes (∼ 200 ng/ml) in hybridization buffer (50% formamide, 5× SSC, 2% blocking reagent, 0.02% SDS, 0.1% N-laurylsarcosine). Hybridized probes were detected using anti-digoxigenin-alkaline phosphatase Fab fragments (3). Sections were incubated in substrate solution for 42 h, then rinsed in TE buffer (10mM Tris, 1mM EDTA, pH 8.0) and mounted in 50% PBS/glycerol.

RT-PCR

Rats were humanely killed, and lungs were excised and immediately submerged in RNAlater (Ambion, Austin, TX). Tissues were stored

TABLE 1. CHARACTERISTICS OF RATS USED FOR PHARMACOKINETIC STUDIES

Characteristics of Rats Used for ^{54}Mn Pharmacokinetic Study			
	Control (n)	Bled (n)	Iron Oxide Aerosol (n)
Body weight, g	356.40 ± 23.63 (10)	308.20 ± 12.49 (10)	331.30 ± 17.08 (10)
Hematocrit, %	51.87 ± 2.28 (6)	44.02 ± 2.22* (6)	49.50 ± 1.31 (6)
Nonheme Fe, μg/g			
Lungs	15.84 ± 4.10 (5)	12.62 ± 3.25 (4)	1,132.34 ± 160.14* (6)
Liver	80.09 ± 10.86 (5)	43.31 ± 6.65* (4)	90.66 ± 14.36 (6)
Brain	13.84 ± 3.22 (5)	12.64 ± 0.62 (4)	13.08 ± 1.20 (6)
Characteristics of Rats Used for ^{59}Fe Pharmacokinetic Study			
	Control (n)	Bled (n)	Iron Oxide–Instilled (n)
Body weight, g	388.46 ± 15.85 (5)	364.28 ± 14.33 (5)	389.92 ± 9.02 (5)
Hematocrit, %	45.01 ± 2.26 (5)	34.30 ± 0.28* (5)	46.09 ± 0.82 (5)
Non-heme Fe, μg/g			
Lungs	29.58 ± 4.28 (3)	20.43 ± 2.34 (3)	1,948.63 ± 327.77* (4)
Liver	79.70 ± 4.62 (5)	ND	127.22 ± 36.47 (5)
Brain	13.80 ± 3.14 (5)	ND	12.80 ± 1.53 (5)

Data are means ± SEM. ND, not determined.
* $P < 0.05$, compared with control.

in RNALater at −20°C until use. RNA was isolated from tissue with RNA-Bee (Tel-Test, Friendswood, TX) following the manufacturer's instructions. RNA was treated with DNase I (Promega, Madison, WI) to remove genomic DNA, then extracted with phenol/chloroform/isoamyl alcohol (25:24:1) mixture, precipitated, resuspended in DEPC-treated water, and quantified by ultraviolet spectrophotometry. cDNA was synthesized from 2 μg lung RNA or 0.5 μg duodenum RNA in reactions containing 1× Moloney murine leukemia virus reverse transcriptase (MMLV-RT) buffer, 0.5 mM dNTP mix, 25 mg/ml Oligo d(T)15 primer, 5 mM $MgCl_2$, 10 mM dithiothreitol, 1 U RNasin, and 200 U MMLV-RT enzyme (Promega). Amplification reactions were carried out with 2 μl cDNA in 1× PCR buffer (10 mM Tris-HCl [pH 9.0], 50 mM KCl, 2.0 mM $MgCl_2$; Promega) with primer sets specific for the 3′ untranslated regions of DMT1-IRE and DMT1-nonIRE isoforms (IRE: forward, 5′-TCCTGCTGAGCGAAGATACC-3′; reverse, 5′-AGACCTCCCCT GACAAAA-3′; non-IRE: forward, 5′-GAACACTTTCTCTAAGC CCT-3′; reverse, 5′-CTTACCCAAACTGGCACG-3′). Fifteen microliters of each reaction was separated on an agarose gel containing ethidium bromide and band intensity was quantified with QuantityOne software (BioRad, Hercules, CA). The relative induction of DMT1 isoforms was normalized to β-actin expression.

Dot Blot Analysis

A human Multiple Tissue Expression (MTE) array was obtained from BDBiosciences Clontech (Palo Alto, CA). The array contains mRNA from 76 different human tissues and cancer cell lines. The radiolabeled probe for human DMT1 was generated by random priming for hybridization to the MTE array blot. After high-stringency washing (2× SSC/0.15% SDS at 60°C), radioactivity was measured by phosphorimaging (Quantity One software; Biorad) to assess expression levels. To normalize the MTE array, the manufacturer has adjusted mRNA loading to reflect band intensity determined for nine different housekeeping genes (β-actin, glyceraldehyde-3-phosphate dehydrogenase, ubiquitin, 23-kD highly basic protein, α-tubulin, phospholipase A2, ribosomal protein S9, transferrin receptor, and hypoxanthine guanine phosphoribosyl transferase).

Statistical Analysis

Pharmacokinetic data are given as means ± SEM. Comparison of control and bled groups and of control and iron oxide exposed groups were evaluated with multivariate analysis of variance (MANOVA) using the GLM (General Linear Model) procedure (SAS statistical analysis software; SAS Institute Inc., Cary, NC). Data for DMT1 mRNA expression by RT-PCR were analyzed using Student's unpaired *t* test to compare control versus bled or iron oxide–exposed groups.

RESULTS

Characteristics of Bled and Iron Oxide–Exposed Rats

The control, bled, and iron oxide–exposed rats used in the study are described in Table 1. The body weights were not significantly different among the three groups. The hematocrits of bled rats and their liver nonheme iron levels were significantly lower than controls. However, iron oxide exposure did not affect hematocrit values. Lung nonheme iron levels were significantly increased by multiple exposures of rats to an aerosol of iron oxide particles or by intratracheal instillations, but nonheme iron levels in other tissues examined did not change.

Pulmonary Effects of Repeated Bleeding or Iron Oxide Exposure

Exposing rats to an inhaled iron oxide aerosol changed the iron content of the lungs and also elicited a modest inflammatory response as reflected by the constituents of BAL fluid (Table 2). Albumin levels in BAL did not change. There was also negligible cell damage or cell death; LDH levels in the BAL supernatant were not significantly elevated. However, there were significant changes in the number of cells present in the lavage fluid. The number of macrophages approximately doubled as a consequence of breathing iron oxide, and the number of neutrophils was elevated by more than an order of magnitude. Repeated bleeding also resulted in an increase in neutrophil numbers, but to a lesser degree. However, it should be noted that few neutrophils degranulated, as indicated by continuing low levels of MPO in all groups. The number of neutrophils observed was also far less than would be seen in exposures to more inflammatory dusts such as alpha quartz (crystalline silica) (18).

TABLE 2. BIOCHEMICAL AND CELLULAR PARAMETERS IN BRONCHOALVEOLAR LAVAGE

	Control	Bled	Iron Oxide Aerosol
Body weight, g	399.50 ± 6.36	308.00 ± 7.02*	370.00 ± 9.39*
Macrophages, millions	13.31 ± 3.43	16.84 ± 1.97	31.91 ± 8.64*
Neutrophils, millions	0.35 ± 0.14	5.44 ± 1.87*	10.60 ± 8.66*
Lymphocytes, millions	0.16 ± 0.07	0.74 ± 0.36	1.04 ± 0.79
LDH, mU/ml	110.88 ± 17.17	146.29 ± 13.91	180.76 ± 81.64
Myeloperoxidase, mU/ml	0.16 ± 0.13	5.01 ± 2.88	1.95 ± 1.63
Albumin, μg	140.74 ± 10.39	281.03 ± 53.02	152.02 ± 40.25

Definition of abbreviation: LDH, lactate dehydrogenase.
Each value is the mean ± SEM of four rats (multivariate ANOVA).
* $P < 0.05$ versus control.

Pharmacokinetics of Intratracheally Instilled ^{54}Mn And ^{59}Fe

The increased levels of iron in the lungs affected the rate of transport of ^{54}Mn or ^{59}Fe from the airways and alveoli to the blood (Figures 1 and 2). In iron oxide–exposed rats, ^{54}Mn levels in the blood during the first 4 h were significantly lower than in untreated controls. Changes in the same direction were seen with ^{59}Fe. Likewise, Fe_2O_3-instilled animals had significantly lower blood levels of ^{59}Fe compared with controls. In contrast, rats made anemic by repeated phlebotomy had significantly higher blood levels of both ^{54}Mn and ^{59}Fe than control rats.

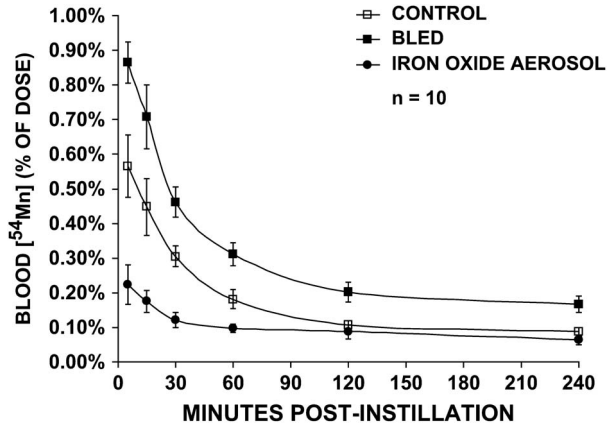

Figure 1. Vascular kinetics of intratracheally instilled ^{54}Mn. Control (*open squares*), bled (*closed squares*), and iron oxide–exposed (*closed circles*) rats were intratracheally instilled with 7.5 μCi/kg $^{54}MnCl_2$. Data are calculated as percentage of the total instilled dose measured in the blood over the first 4 h. Significantly less ^{54}Mn was detected in the blood in iron oxide aerosol–exposed rats (MANOVA, $P < 0.0001$). In contrast, significantly more ^{54}Mn was found in the blood of bled rats (MANOVA, $P < 0.0001$), although the slope was not different from control. The blood levels significantly decreased over time in all three groups of rats (MANOVA, $P < 0.0001$).

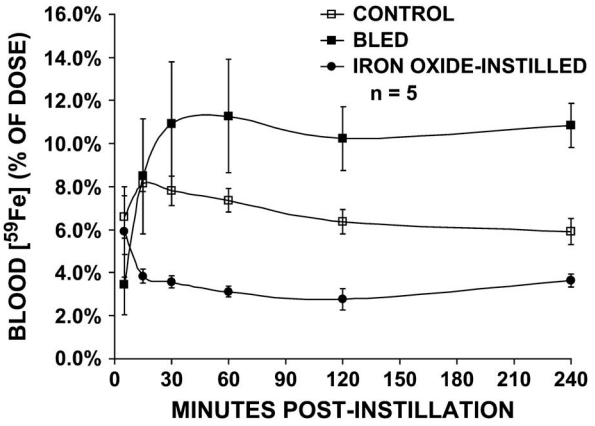

Figure 2. Vascular kinetics of intratracheally instilled ^{59}Fe. Control (*open squares*), bled (*closed squares*), and iron oxide–exposed (*closed circles*) rats were intratracheally instilled with 22 μCi/kg $^{59}FeCl_3$. Data are calculated as percentage of the total instilled dose detected in the blood over the first 4 h. As with ^{54}Mn, significantly less ^{59}Fe was found in the blood in iron oxide–instilled but more in bled rats (MANOVA, $P < 0.05$). The kinetics of pulmonary absorption of ^{59}Fe was different from ^{54}Mn. The percentage of ^{59}Fe in the blood was ∼ 10 times more than that of ^{54}Mn in normal rats. The shape of the blood kinetic curve was also different with an initial delay in ^{59}Fe peak values from 5–15 min compared to ^{54}Mn.

Levels of radioactive metals measured in the blood reflect not only rates of transport into the blood, but also their rate of removal from the blood by organs and tissues. The amount of radioisotope remaining in the lungs at times of killing reflects the extent of metal clearance from the lungs. Significantly more ^{54}Mn was retained in the lungs of Fe_2O_3 aerosol-exposed rats at 4 and 72 h than controls, confirming that pulmonary transport was attenuated by higher local iron levels (Tables 3 and 4). The same change was observed with ^{59}Fe in Fe_2O_3-instilled rats. However, bled rats also retained significantly more ^{59}Fe in the lungs despite higher levels in the blood (Table 5), showing that these higher levels reflect decreased vascular clearance rather than enhanced pulmonary transport.

TABLE 3. DISTRIBUTION OF ^{54}Mn IN TISSUES 4 h AFTER INTRATRACHEAL INSTILLATION OF $^{54}MnCl_2$ IN RATS EXPOSED TO IRON OXIDE AEROSOL AND IN REPEATEDLY BLED RATS

	4 h after Instillation		
	Control	Bled	Iron Oxide Aerosol
Lungs	57.366 ± 3.623	58.068 ± 2.218	73.765 ± 2.402†
Blood	0.089 ± 0.023	0.159 ± 0.036	0.062 ± 0.019
Liver	4.965 ± 1.495	4.547 ± 2.106	2.255 ± 0.826
Heart	0.415 ± 0.039	0.471 ± 0.023	0.189 ± 0.012†
Brain	0.054 ± 0.008	0.078 ± 0.005*	0.030 ± 0.001†
Spleen	0.232 ± 0.031	0.291 ± 0.044	0.114 ± 0.005†
Kidneys	3.120 ± 0.256	3.261 ± 0.269	1.372 ± 0.089†
Stomach	0.629 ± 0.177	0.835 ± 0.232	1.081 ± 0.605
Small Intestine	6.519 ± 1.168	5.569 ± 1.386	4.233 ± 1.203
Large Intestine	2.505 ± 0.552	3.530 ± 0.815	1.578 ± 0.626
Urine	0.019 ± 0.008	0.009 ± 0.005	0.001 ± 0.000
Feces	0.002 ± 0.002	0.008 ± 0.006	0.028 ± 0.013

Values represent radioactivity (% of total instilled dose).
Each value is the mean ± SEM of five rats (multivariate ANOVA).
* $P < 0.05$ control versus bled.
† $P < 0.05$ control versus iron oxide aerosol.

TABLE 4. DISTRIBUTION OF ^{54}Mn IN TISSUES 72 h AFTER INTRATRACHEAL INSTILLATION OF $^{54}MnCl_2$ IN RATS EXPOSED TO IRON OXIDE AEROSOL AND IN REPEATEDLY BLED RATS

	72 h after Instillation		
	Control	Bled	Iron Oxide Aerosol
Lungs	20.015 ± 1.901*	25.032 ± 1.813*	35.991 ± 2.716*†
Blood	0.118 ± 0.026	0.118 ± 0.024	0.083 ± 0.019
Liver	7.753 ± 1.529	6.884 ± 0.845	7.216 ± 0.574*
Heart	0.209 ± 0.008*	0.209 ± 0.004*	0.170 ± 0.018
Brain	0.121 ± 0.024*	0.167 ± 0.006*	0.167 ± 0.041*
Spleen	0.164 ± 0.030	0.189 ± 0.025	0.183 ± 0.007*
Kidneys	2.989 ± 0.587	3.300 ± 0.253	2.701 ± 0.082*
Stomach	0.501 ± 0.119	0.535 ± 0.111	0.457 ± 0.088
Small Intestine	2.124 ± 0.529	2.378 ± 0.327	2.601 ± 1.128
Large Intestine	5.111 ± 0.712*	4.976 ± 0.978	2.937 ± 0.327
Urine	0.029 ± 0.008	0.033 ± 0.017	0.026 ± 0.006*
Feces	24.945 ± 7.775	22.119 ± 4.162*	20.717 ± 2.778*

Values represent radioactivity (% of total instilled dose).
Each value is the mean ± SEM of five rats (multivariate ANOVA).
* $P < 0.05$, 72 h versus 4 h.
† $P < 0.05$ control versus iron oxide aerosol.

In addition, the extent of absorption of ^{54}Mn versus ^{59}Fe from the lungs was very different. Sustained blood levels after absorption of ^{59}Fe through the lungs were greater than that for ^{54}Mn on a % of instilled dose basis (< 1% instilled dose for ^{54}Mn compared with 2–12% instilled dose for ^{59}Fe). The time course of metal transport as reflected in the shape of the blood level curves also differed. ^{54}Mn blood levels were highest in all rats for the first time point. For ^{59}Fe, there was a delay of ∼ 15 min in control and bled rats before reaching maximal values. Once a plateau was reached at 30 min, blood levels of ^{59}Fe remained unchanged over the next 3.5 h.

Tissue Uptake of ^{54}Mn and ^{59}Fe

The tissue distributions of ^{54}Mn are summarized in Tables 3–5. The amount of ^{54}Mn retained in the lungs at 4 h (Table 3) or 72 h (Table 4) in iron oxide–exposed rats was significantly higher

TABLE 5. DISTRIBUTION OF ^{59}Fe IN TISSUES 4 h AFTER INTRATRACHEAL INSTILLATION OF ^{59}Fe IN REPEATEDLY BLED RATS OR RATS INSTILLED WITH IRON OXIDE PARTICLE SUSPENSION

	4 h after Instillation		
	Control	Bled	Iron Oxide–Instilled
Lungs	48.43 ± 2.056	64.749 ± 4.134*	54.763 ± 0.594†
Blood	5.913 ± 0.597	10.843 ± 1.025*	3.650 ± 0.296†
Liver	2.944 ± 0.451	1.781 ± 0.160*	1.411 ± 0.139†
Heart	0.116 ± 0.039	0.072 ± 0.009	0.057 ± 0.008
Brain	0.053 ± 0.025	0.008 ± 0.006	0.012 ± 0.001
Spleen	0.398 ± 0.078	1.423 ± 0.330*	0.187 ± 0.033†
Kidneys	1.852 ± 1.488	0.166 ± 0.026	0.217 ± 0.023
Stomach	0.418 ± 0.082	0.877 ± 0.417	0.092 ± 0.013†
Small Intestine	1.743 ± 0.364	0.926 ± 0.132	0.809 ± 0.178†
Large Intestine	0.144 ± 0.037	0.479 ± 0.259	0.100 ± 0.022
Urine	0.022 ± 0.003	0.018 ± 0.008	0.321 ± 0.148
Feces	0.002 ± 0.001	0.006 ± 0.006	0.001 ± 0.001
Total	76.099 ± 8.075	85.807 ± 1.329	64.988 ± 0.254

Values represent radioactivity (% of total instilled dose).
Each value is the mean ± SEM of five rats (multivariate ANOVA).
* $P < 0.05$ control versus bled.
† $P < 0.05$ control versus iron oxide aerosol.

than in controls. This suggests a slower rate of transport of radioactive manganese from the alveoli to the blood, a result consistent with pharmacokinetic data (Figure 1). At 4 h, uptake of ^{54}Mn by other organs was significantly decreased in the heart, brain, spleen, kidneys, skeletal muscle, and bone marrow by iron oxide exposure. The radioisotope levels of these tissues significantly increased over time (from 4 to 72 h) and at 72 h were no longer different from control values. The tissue distribution of ^{59}Fe was significantly altered in iron oxide–instilled rats at 4 h, the only time point measured (Table 5). More ^{59}Fe remained in the lungs and significantly less was found in blood, liver, spleen, stomach, and small intestine.

Although bled rats retained the same amount of ^{54}Mn in the lungs, they accumulated significantly more radioisotope in the brain. Significantly more ^{59}Fe remained in the lungs of bled rats. Higher levels of ^{59}Fe in the lungs at 4 h, and elevated blood levels (Figure 2), suggest that these animals absorbed significantly less ^{59}Fe through the lungs, and at the same time cleared ^{59}Fe more slowly from the blood. Significantly less ^{59}Fe accumulated in the liver while increased levels were observed in the spleen of bled rats, consistent with mobilization of iron stores for enhanced erythropoiesis (19).

DMT1 Is Abundantly Expressed in Human Lungs

To evaluate the relative expression level of DMT1 in the lungs, we conducted a dot blot analysis comparing several human tissues using an MTE array (Clontech). Relative DMT1 expression levels were assessed by quantifying the amount of radiolabeled probe hybridized by phosporimaging. As shown in Figure 3, the level of DMT1 mRNA in human lung is high relative to several other tissues (heart, esophagus, colon, kidney, liver). Although previous studies identified expression of DMT1 mRNA in the rat lung (3) and in a human bronchial epithelium–derived cell line (20), our data further show that the lungs are a site of abundant expression of this transporter in humans.

DMT1 Expression in Rat Lungs

In situ hybridization showed that DMT1 is expressed in normal rat airway and alveolar epithelium, especially type II cells (Figures 4A and 5A). No significant overall change in DMT1 expression was observed in lungs from bled rats (Figure 4C). However, iron oxide exposure is associated with local up-regulation of DMT1 in areas where particle-containing macrophages were found (Figure 4B). In those areas, we saw significantly more DMT1-related staining in the instilled animals compared with control animals. That the presence of iron oxide is causally related to increased DMT1 mRNA expression is also suggested by Figure 5. Because intratracheal instillation of particles leads to nonuniform distribution (12), some regions of the lungs have few or no particles while other areas have significant numbers. In regions of the lung where few particles are seen, we detected very little DMT1 mRNA (Figure 5B). In contrast, areas of the

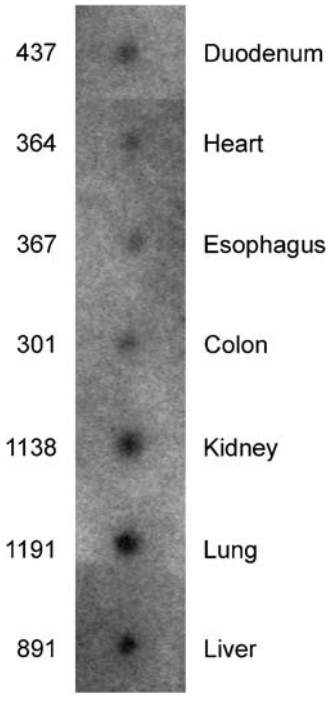

Figure 3. DMT1 expression in human tissues. Human MTE blot probed for DMT1 mRNA. A human MTE blot (Clontech) was probed with a randomly primed 32P-labeled 1.1-kb fragment of human DMT1 (non–isoform-specific). Loading of mRNA was normalized by the manufacturer to several housekeeping genes (β-actin, glyceraldehyde 3′-phosphate dehydrogenase, ubiquitin, 23-kD highly basic protein, β-tubulin, phospholipase A2, ribosomal protein S9, transferrin receptor, and hypoxanthine guanine phosphorbiosyl transferase). Radioactivity was measured by phosphorimaging; shown are phosphor counts quantified using Quantity One software (BioRad).

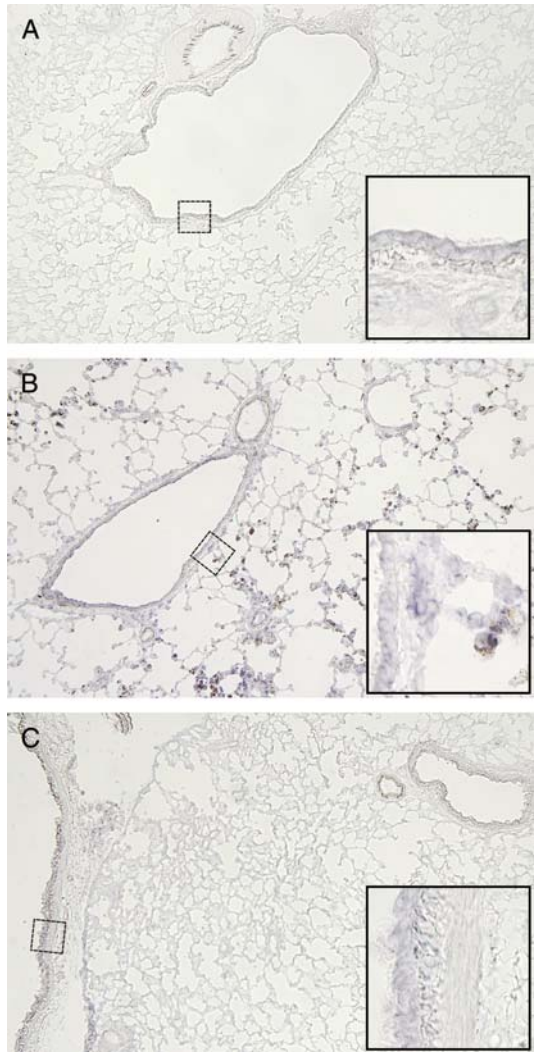

Figure 4. DMT1 expression in rat lungs. *In situ* hybridization for DMT1 in control, repeatedly bled, and iron oxide–instilled rat lungs. Ten-micrometer-thick lung cryosections embedded in O.C.T. compound (TissueTek, Hatfield, PA) were hybridized with digoxigenin-labeled sense and antisense transcripts transcribed off of a 900 bp DMT1 cDNA fragment (bases 1–654). Transcripts were truncated to ~200–400 bp by alkali-hydrolysis. Hybridized probe was detected using anti-digoxigenin Fab fragments (Roche, Indianapolis, IN) and BCIP/NBT substrate. *Bluish-purple staining* reflects mRNA of DMT1, while iron oxide particles appear *brown* (nominal magnification ×4). (*A*) Control rat lung. Only very faint DMT1 staining is evident. (*B*) A section of rat lung that received iron oxide particles by instillation. (*C*) Bled rat lung.

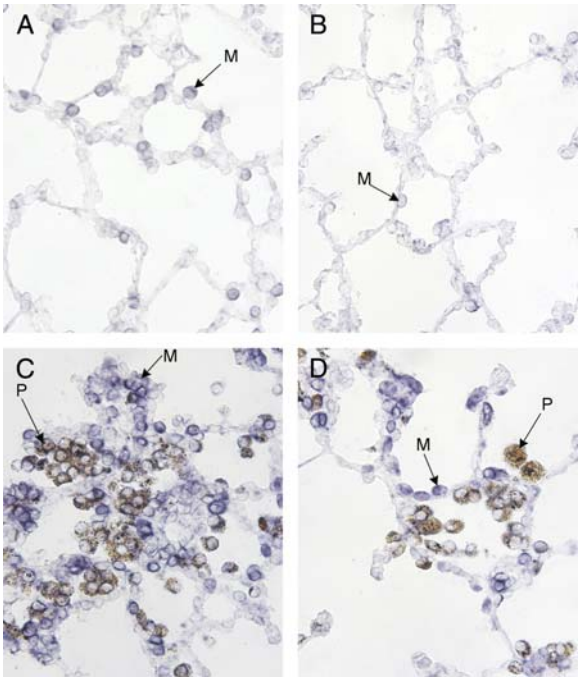

Figure 5. DMT1 expression in rat lungs. *In situ* hybridization for DMT1 in control and iron oxide–instilled rat lungs at higher magnification (×25). (*A*) Control rat lung. (*B*) Lung section from an animal instilled with iron oxide particles from a region where few particles were found. (*C* and *D*) Lung section from an iron oxide particle–instilled rat from regions of particle retention (nominal magnification ×25). M, macrophage; P, macrophage with phagocytized particles.

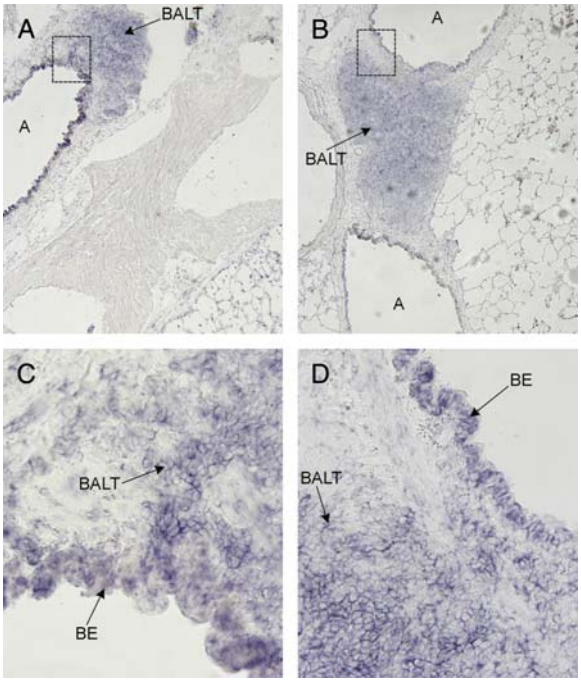

Figure 6. DMT1 expression in rat lungs. *In situ* hybridization for DMT1 in control and iron oxide–instilled rat lungs with large airways (A) and blood vessels. (*A*) Lung sections from control rat (inset is in *C*). (*B*) Lung sections from iron oxide–instilled rat (inset is in *D*). In both control and exposed rats, there is intense staining for DMT1 in bronchial epithelial cells (BE). Also shown are examples of BALT with staining for DMT1. Images shown are at ×4 magnification; *insets* (*C* and *D*) are also shown at ×25.

same lung where many particles are deposited demonstrate local recruitment of macrophages to that area, and a significant upregulation of DMT1 mRNA in those cells and in adjacent epithelial regions (Figures 5C and 5D).

Blood vessels generally showed little DMT1 expression (Figure 6A). In contrast, large airways showed extensive staining (Figures 6A and 6B). DMT1 mRNA expression was also observed in bronchus-associated lymphoid tissue (BALT) adjacent to large airways. However, in large airways and BALT there was no discernable difference between control and iron oxide–exposed rats (Figures 6C and 6D). DMT1 expression in bled rat lungs as determined by *in situ* hybridization did not differ from that of controls. In lung tissues, two mRNA splice variants of DMT1 transcribed from the same gene are expressed (21). The splice variants differ only in their 3′ untranslated regions; one contains an iron-responsive element (IRE) while the other does not (21). By RT-PCR, we found no difference in expression level of either isoform in lungs of bled rats (Figure 7).

DISCUSSION

Our pharmacokinetic experiments on the clearance of soluble iron and manganese in the lungs examined the effects of local iron loading of the lungs and of systemic iron deficiency induced by repeated phlebotomy. At 4 h, transport of both ^{59}Fe and ^{54}Mn from the lungs was suppressed in iron oxide–exposed rats. This observation might be explained by the presence of large amounts of soluble iron cations that compete with instilled radioisotope for a finite amount of transport protein, such as DMT1. Other metal transport systems such as the transferrin–transferrin receptor system would also be susceptible to such competitive inhibition. The dramatic increases in nonheme iron observed in the lungs suggest that maximum transport of iron and manganese ions may have been approached or perhaps even attained at some sites. An alternative possibility is the downregulation of transport systems by increased iron. However, we observed local upregulation of DMT1 mRNA in iron oxide–instilled rats and, although our attempt to detect DMT1 protein expression using commercially available antisera was unsuccessful, Wang and coworkers (20) have shown that non-IRE DMT1 protein is upregulated in rat lung epithelium after instillation of ferric ammonium citrate. Therefore, we favor the idea that competitive inhibition is the dominant mechanism involved in the suppression of pulmonary transport.

Decreased pulmonary transport of ^{54}Mn in iron oxide–exposed rats resulted in reduced uptake by other organs, including heart, brain, spleen, kidneys, skeletal muscle, and bone marrow. Likewise, significantly less ^{59}Fe was found in blood, liver, spleen, stomach, and small intestine of iron oxide–exposed rats. Thus, inhalation of iron oxide particles correlated with decreased accumulation of the intratracheally instilled metals in other critical organs. In contrast, phlebotomy-induced anemia was associated with higher blood levels of both ^{54}Mn and ^{59}Fe. This effect was not due to enhanced pulmonary transport of metals, since levels of ^{54}Mn remaining in the lungs of control and bled rats at 4 h were the same. In fact, the lung level of ^{59}Fe was significantly higher in bled than in control rats. The elevated levels of circulating ^{54}Mn and ^{59}Fe observed in bled rats, therefore, appear to be due to decreased clearance of these metals from the blood.

Increased blood levels of instilled ^{54}Mn in anemic bled rats resulted in significantly more brain uptake of the metal compared with control animals. This trend increased over time (72 h versus

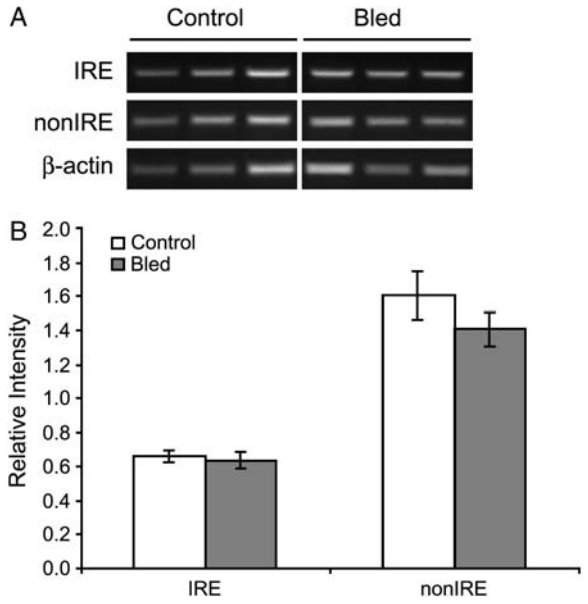

Figure 7. DMT1 expression in rat lungs. Semiquantitative RT-PCR with isoform specific primers for DMT1 mRNA in repeatedly bled and control rats. To determine if isoform-specific changes in DMT1 mRNA levels can be detected, semiquantitative RT-PCR was performed on total RNA isolated from bled and control rat lungs (*A*). Isolation of total RNA from iron oxide instilled rats was unsuccessful due to technical problems. (*B*) Relative intensities of isoform specific RT-PCR products were not different between bled and control rat lungs. (n = 3 rats per group).

4 h). Our finding that phlebotomy-induced anemia enhances brain manganese uptake is consistent with previous studies demonstrating increased brain manganese uptake after intravenous injection of rats made iron-deficient by diet (22, 23). In the case of ^{59}Fe, the elevated blood levels in anemic rats resulted in increased retention in the spleen but reduced liver levels, consistent with increased mobilization of iron stores for erythropoiesis (19). These results indicate that anemia due to chronic blood loss can dramatically change the tissue distribution and deposition of inhaled metals, and may predispose an individual to manganese neurotoxicity.

Lung injury and inflammation might also influence manganese or iron transport from the airways and alveoli to the blood. To examine this possibility, we determined the effects of repeated exposure to iron oxide aerosol or repeated bleeding on lung injury and/or inflammation. Our data indicate that repeated inhalation of Fe_2O_3 caused modest increases in macrophages and neutrophils (Table 2). Deposition of increased particles in the lungs, which are cleared via phagocytic mechanisms, would promote increased numbers of macrophages. During infection or increased numbers of deposited particles, macrophages can be supplemented by migration of neutrophils from the blood to the alveolar spaces. In comparison to instilled iron oxide, however, other particles such as silica elicit many more neutrophils (18). Also in contrast to many other toxic dusts that promote 10- to 20-fold increases in LDH (18), a significant change in LDH levels with iron oxide exposure was not observed. Finally, it seems reasonable that significant inflammation might increase removal of ^{54}Mn and ^{59}Fe from the lungs; in fact, we observed a decrease. Thus, it is unlikely that our pharmacokinetic data reflect strong influences due to lung injury or inflammation.

DMT1 expression has been shown to increase in bronchial epithelial cells in response to inflammatory stimuli (24), but this effect should enhance rather than attenuate metal absorption. While local upregulation of DMT1 mRNA was observed in iron oxide–instilled rats, overall transport of ^{54}Mn or ^{59}Fe across the air–blood barrier was not enhanced. In bled rats, DMT1 expression in lungs was not different from that in controls, and differences in the clearance of ^{54}Mn and ^{59}Fe from circulation appear to account for the increased blood levels observed in our study. Thus, DMT1 does not seem to be rate limiting for pulmonary clearance of these metals, although it is possible that this transport protein contributes to other lung-associated functions. For example, DMT1 in macrophages could operate at the level of the macrophage phagolysosome. As described by Kreyling and colleagues (25), export of solubilized metal from phagolysosomes might maintain a concentration gradient for dissolution of particles. Thus, increased levels of DMT1 may be related to optimizing particle dissolution rates within phagocytic cells, but have little to do with metal transport across the air–blood barrier. The presence of DMT1 could also help promote iron storage in the pulmonary epithelium. It has been shown that iron oxide inhalation is followed by significant increases in ferritin and hemosiderin within epithelial cells (26). The strong staining of DMT1 in BALT suggests that metals accumulate in this region as well.

In summary, iron oxide exposure significantly reduces pulmonary transport of manganese and iron, resulting in decreased uptake by other critical organs. Phlebotomy-induced anemia is also associated with reduced transport of iron from the lungs to the blood, but manganese absorption is unaffected. However, blood clearance of both metals is reduced in phlebotomized animals, leading to increased tissue exposure and greater retention of manganese in the brain and iron in the spleen. Although DMT1 is present in rat and human lungs, it does not appear to be associated with the observed changes in pulmonary absorption of iron and manganese in iron oxide–exposed or bled rats. Since environmental sources of metals are usually found in complex particles, and since chronic exposure to high levels of manganese can lead to neurological disorders, increased knowledge about iron status and the cellular and molecular basis of metal transport may suggest preventive and therapeutic approaches to reduce the toxicity of metals.

Conflict of Interest Statement: J.D.B. received $70,361.50 between 1999 and 2002 from the American Welding Society in the form of a gift to Harvard University. E.H. does not have a financial relationship with a commercial entity that has an interest in the subject of this manuscript. T.C.D. does not have a financial relationship with a commercial entity that has an interest in the subject of this manuscript. M.D.K. does not have a financial relationship with a commercial entity that has an interest in the subject of this manuscript. M.W.-R. does not have a financial relationship with a commercial entity that has an interest in the subject of this manuscript. R.M.M. does not have a financial relationship with a commercial entity that has an interest in the subject of this manuscript.

Acknowledgments: The authors thank Krishna Murthy for help in exposure of rats to aerosol of iron oxide particles.

References

1. Lucchini R, Apostoli P, Perrone C, Placidi D, Albini E, Migliorati P, Mergler D, Sassine MP, Palmi S, Alessio L. Long-term exposure to "low levels" of manganese oxides and neurofunctional changes in ferroalloy workers. *Neurotoxicology* 1999;20:287–297.
2. Mergler D, Baldwin M, Belanger S, Larribe F, Beuter A, Bowler R, Panisset M, Edwards R, de Geoffroy A, Sassine MP, *et al.* Manganese neurotoxicity, a continuum of dysfunction: results from a community based study. *Neurotoxicology* 1999;20:327–342.
3. Gunshin H, Mackenzie B, Berger UV, Gunshin Y, Romero MF, Boron WF, Nussberger S, Gollan JL, Hediger MA. Cloning and characterization of a mammalian proton-coupled metal-ion transporter. *Nature* 1997; 388:482–488.
4. Garrick MD, Dolan KG, Horbinski C, Ghio AJ, Higgins D, Porubcin M, Moore EG, Hainsworth LN, Umbreit JN, Conrad ME, *et al.* DMT1: a mammalian transporter for multiple metals. *Biometals* 2003;16:41–54.

5. Trinder D, Oates PS, Thomas C, Sadleir J, Morgan EH. Localisation of divalent metal transporter 1 (DMT1) to the microvillus membrane of rat duodenal enterocytes in iron deficiency, but to hepatocytes in iron overload. *Gut* 2000;46:270–276.
6. Davis CD, Wolf TL, Greger JL. Varying levels of manganese and iron affect absorption and gut endogenous losses of manganese by rats. *J Nutr* 1992;122:1300–1308.
7. Aschner M, Aschner JL. Manganese neurotoxicity: cellular effects and blood-brain barrier transport. *Neurosci Biobehav Rev* 1991;15:333–340.
8. Mena I, Horiuchi K, Lopez G. Factors enhancing entrance of manganese into brain: iron deficiency and age [abstract]. *J of Nuc Med* 1974;15:516.
9. Turi JL, Yang F, Garrick MD, Piantadosi CA, Ghio AJ. The iron cycle and oxidative stress in the lung. *Free Radic Biol Med* 2004;36:850–857.
10. Chua AC, Morgan EH. Manganese metabolism is impaired in the Belgrade laboratory rat. *J Comp Physiol B Biochem System Environ Physiol* 1997;167:361–369.
11. Valberg PA, Brain JD. Generation and use of three types of iron-oxide aerosol. *Am Rev Respir Dis* 1979;120:1013–1024.
12. Brain JD, Knudson DE, Sorokin SP, Davis MA. Pulmonary distribution of particles given by intratracheal instillation or by aerosol inhalation. *Environ Res* 1976;11:13–33.
13. Torrance JD, Bothwell TH. A simple technique for measuring storage iron concentrations in formalinised liver samples. *S Afr J Med Sci* 1968; 33:9–11.
14. Beck BD, Brain JD, Bohannon DE. An in vivo hamster bioassay to assess the toxicity of particulates for the lungs. *Toxicol Appl Pharmacol* 1982;66:9–29.
15. Fairman E, Corner G. The bone-marrow volume of the albino rat. *Anat Rec* 1933;60:1–4.
16. Fairman E, Whipple G. Bone-marrow volume in adult dogs. *Am J Physiol* 1934;104:352–357.
17. Diluzio NR, Zilversmit DB. Influence of exogenous proteins on blood clearance and tissue distribution of colloidal gold. *Am J Physiol* 1955; 180:563–565.
18. Brain JD, Long NC, Wolfthal SF, Dumyahn T, Dockery DW. Pulmonary toxicity in hamsters of smoke particles from Kuwaiti oil fires. *Environ Health Perspect* 1998;106:141–146.
19. Burkhard MJ, Brown DE, McGrath JP, Meador VP, Mayle DA, Keaton MJ, Hoffman WP, Zimmermann JL, Abbott DL, Sun SC. Evaluation of the erythroid regenerative response in two different models of experimentally induced iron deficiency anemia. *Vet Clin Pathol* 2001; 30:76–85.
20. Wang X, Ghio AJ, Yang F, Dolan KG, Garrick MD, Piantadosi CA. Iron uptake and Nramp2/DMT1/DCT1 in human bronchial epithelial cells. *Am J Physiol Lung Cell Mol Physiol* 2002;282:L987–L995.
21. Lee PL, Gelbart T, West C, Halloran C, Beutler E. The human Nramp2 gene: characterization of the gene structure, alternative splicing, promoter region and polymorphisms. *Blood Cells Mol Dis* 1998;24:199–215.
22. Heilig E, Molina R, Donaghey T, Brain JD, Wessling-Resnick M. Pharmacokinetics of pulmonary manganese absorption: evidence for increased susceptibility to manganese loading in iron-deficient rats. *Am J Physiol Lung Cell Mol Physiol* 2005;288:L887–L893.
23. Chua AC, Morgan EH. Effects of iron deficiency and iron overload on manganese uptake and deposition in the brain and other organs of the rat. *Biol Trace Elem Res* 1996;55:39–54.
24. Wang X, Garrick MD, Yang F, Dailey LA, Piantadosi CA, Ghio AJ. TNF, IFN-{gamma}, and endotoxin increase expression of DMT1 in bronchial epithelial cells. *Am J Physiol Lung Cell Mol Physiol* 2005; 289:pL24–pL33.
25. Kreyling WG, Godleski JJ, Kariya ST, Rose RM, Brain JD. *In vitro* dissolution of uniform cobalt oxide particles by human and canine alveolar macrophages. *Am J Respir Cell Mol Biol* 1990;2:413–422.
26. Watson AY, Brain JD. Uptake of iron aerosols by mouse airway epithelium. *Lab Invest* 1979;40:450–459.